

Numerical simulation of wave slamming on 3D offshore platform deck using a coupled Level-Set and Volume-of-Fluid method for overset grid system

Yucheng Zhao^{*1}, Hamn-Ching Chen¹ and Xiaochuan Yu²

¹Zachry Department of Civil Engineering, Texas A&M University, College Station, TX 77843-3136, USA

²School of Naval Architecture & Marine Engineering, College of Engineering, The University of New Orleans, New Orleans, LA 70148, USA

(Received October 28, 2015, Revised November 26, 2015, Accepted November 30, 2015)

Abstract. The numerical simulation of wave slamming on a 3D platform deck was investigated using a coupled Level-Set and Volume-of-Fluid (CLSVOF) method for overset grid system incorporated into the Finite-Analytic Navier-Stokes (FANS) method. The predicted slamming impact forces were compared with the corresponding experimental data. The comparisons showed that the CLSVOF method is capable of accurately predicting the slamming impact and capturing the violent free surface flow including wave slamming, wave inundation and wave recession. Moreover, the capability of the present CLSVOF method for overset grid system is a prominent feature to handle the prediction of wave slamming on offshore structure.

Keywords: computational fluid dynamics; CLSVOF; overset grid; slamming; fluid-structure interaction

1. Introduction

Wave induced loads on offshore structures are crucial for both the design and the operation of these structures. The impulse loads with large pressure peaks can occur when extreme waves inundate the deck of offshore structures. These loads acting upon the deck are called “slamming” forces. Different from other wave loads, slamming loads happen in much localized space, and in very short time. The impulsive slamming loads may cause damage to the horizontal decks of offshore structure or lead to the collapse of the whole structure. Moreover, the magnitude of the slamming impact load is particularly uncertain and difficult to predict. Hence, it is necessary to investigate slamming forces on offshore structures.

The experimental and numerical investigations relating to wave slamming on offshore structures have been studied over several decades. Wang (1970) developed the theoretical technique to predict for both the slow-rise pressure component and the impact components for different incident waves. Broughton and Horn (1987) used wave basin tests to measure vertical forces applied underneath the platform. Kaplan (1992) presented an analytical solution to determine the time history of the slamming forces acting on horizontal deck structures. Kaplan *et*

*Corresponding author, Ph.D., E-mail: zhaoyucc@tamu.edu

al. (1995) also extended the research to predict the wave impact forces and the horizontal forces acting on offshore deck structures during large incident waves. Iwanowski *et al.* (2002) computed the impact loads, through a solution of complete Navier-Stokes equations, with the VOF method. Ren and Wang (2004) presented the investigation of random wave slamming on structures in the splash zone by the VOF method. Bunnik and Buchner (2007) applied the improved volume of fluid (iVOF) method to predict the extreme wave effects on floating deep-water structures. Chen and Yu (2009) employed the Level-Set Navier-Stokes method for the simulation of X-craft wet deck slamming in pitch and heave motions. Chen (2010, 2012) used the Level-Set Navier-Stokes method to simulate hurricane wave loads on a fixed offshore platform and a jack-up structure. Gao *et al.* (2012) investigated regular wave slamming on an open-piled structure by Smoothed Particle Hydrodynamics (SPH) method.

It can be concluded that the numerical method is a potential tool in the application of wave slamming on offshore structures. The Smoothed Particle Hydrodynamics (SPH) method, the Volume-of-Fluid (VOF) method and the Level-Set (LS) method have been successfully applied to capture the interface profile in an event of wave slamming on offshore structure. However, each of single method has its own advantages and disadvantages. Although the SPH method can achieve high accuracy, it requires large number of particles to produce the simulations. The VOF method has a good mass conservation property, but it lacks accuracy for the calculations of interface normal and curvature. In the LS method, the interface normal and curvature can be accurately calculated from the continuous and smooth LS function. However, the LS method is not able to preserve mass conservation. To overcome these weaknesses, a coupled Level-Set and Volume-of-Fluid (CLSVOF) method was proposed by Sussman and Puckett (2000). In the CLSVOF method, the interface is reconstructed from the VOF method to preserve the mass conservation and the geometric properties are evaluated by the LS method. Recently, a new CLSVOF method for overset grid system was developed by Zhao and Chen (2013, 2014). The Chimera domain decomposition approach was implemented in the CLSVOF method for overset grid system including embedding, overlapping and matching grids.

In the present study, the CLSVOF method for overset grid system of Zhao and Chen (2013, 2014) is employed as the interface-capturing method and incorporated into the Finite-Analytical Navier-Stokes (FANS) method (Chen *et al.* 1990, Chen and Yu 2009, Chen 2011) for time-domain simulation of wave slamming on 3D offshore platform. The present CLSVOF method was validated by Zhao and Chen (2014, 2015) for several benchmark cases and applications including the Zalesak's problem, the stretching of a circular fluid element, and the 3D sloshing flow in partially filled LNG tank. In this study, an overset grid system is utilized to facilitate the simulation of complex flow around the platform deck. The complex free surface flow patterns as well as deck local pressure contours are captured by the present CLSVOF method. The regular wave slamming total impact loads on the underside of the structure are calculated from the numerical results, and also verification with the experimental results.

2. Governing equations

In the Level-Set formulation (Osher and Sethian 1988), the LS function ϕ is defined as a signed distance from the interface. The value is zero on an interface, negative in air, and positive in liquid. In the VOF formulation (Hirt and Nichols 1981), the VOF function C represents the volume fraction of liquid phase in a computational cell. Its value is between zero and one in cells cut by

interface. The values are zero or one where the cells are away from interface. The LS and VOF functions are advected in the local velocity field \bar{V} during time t by solving Eqs. (1) and (2), respectively.

$$\frac{\partial \phi}{\partial t} + \bar{V} \cdot \nabla \phi = 0 \tag{1}$$

$$\frac{\partial C}{\partial t} + \bar{V} \cdot \nabla C = 0 \tag{2}$$

The geometric properties such as interface normal \bar{m} and curvature κ can be accurately calculated from the LS function,

$$\bar{m} = \frac{\nabla \phi}{|\nabla \phi|} \quad \kappa = \nabla \cdot \frac{\nabla \phi}{|\nabla \phi|} \tag{3}$$

In the present two-phase flow formulation, both the density ρ and the viscosity μ nearby the interface depend on the LS function. The region where both the density and the viscosity vary is defined as a transition zone. And the transition zone is defined by $|\phi| \leq \varepsilon$, where ε is the half thickness of the interface. In the transition of the interface, the fluid properties, such as non-dimensional density $\rho(\phi)$ and non-dimensional dynamic viscosity $\mu(\phi)$, can be smoothed by the smoothed Heaviside function.

$$\begin{cases} \rho(\phi) = \rho_a / \rho_l + (1 - \rho_a / \rho_l) \cdot H(\phi) \\ \mu(\phi) = \mu_a / \mu_l + (1 - \mu_a / \mu_l) \cdot H(\phi) \end{cases} \tag{4}$$

where the subscripts a and l represent air and liquid phases; the smoothed Heaviside function is specified as

$$H(\phi) = \begin{cases} 0 & \text{if } \phi < -\varepsilon \\ \frac{1}{2} \left(1 + \frac{\phi}{\varepsilon} + \frac{1}{\pi} \sin\left(\frac{\pi\phi}{\varepsilon}\right) \right) & \text{if } -\varepsilon \leq \phi \leq \varepsilon \\ 1 & \text{if } \phi > \varepsilon \end{cases} \tag{5}$$

It is assumed that both water and air are governed by the incompressible Navier-Stokes equations in the following form

$$\frac{\partial \bar{V}}{\partial t} + \bar{V} \cdot \nabla \bar{V} = -\frac{\delta_{i,3}}{Fr^2} + \frac{\nu(\phi)}{Re} \nabla^2 \bar{V} - \frac{1}{\rho(\phi)} \nabla p \tag{6}$$

where $\delta_{i,j}$ is the Kronecker delta function, $\nu(\phi) = \mu(\phi) / \rho(\phi)$ is the non-dimensional kinematic viscosity, p is pressure, Fr is Froude number and Re is Reynolds number.

In the present study, the continuity and momentum equations for the two-phase flow are solved in curvilinear coordinates using the finite-analytical method of Chen *et al.* (1990). The LS advection equation Eq. (1) is solved using the third order TVD Runge-Kutta scheme for temporal derivative and the fifth-order WENO scheme for spatial derivatives. The VOF advection equation Eq. (2) is performed using the PLIC interface reconstruction and the mixed Lagrangian and

Eulerian advection scheme. More details of the CLSVOF method for overset grid system can be found in Zhao and Chen (2013, 2014).

3. Experimental and numerical setups

The wave slamming impact experimental data adopted for comparison purposes were measured by Ren *et al.* (2007). In the experiment, the wave channel is 50.0 m in length, 3.0 m in width, 1.0 m in height and the water depth is 0.5 m. The platform deck model is designed as 60.0 cm long, 60.0 cm wide and 2.0 cm thick. The clearance of the underside of the structure above the mean water level s is 0.02 m. A cluster of 16 pressure transducers are mounted on the underside of the deck to measure the slamming impact pressure, as illustrated in Fig. 1. The sampling frequency of all the pressure transducers is about 500Hz. The direction of regular incident wave propagation β is defined in Fig. 2 and chosen to be 0° , 15° , 30° and 45° . The regular incoming wave height H is 10.0 cm, the wave period T is 1.0s, and the wave length L is 1.512 m.

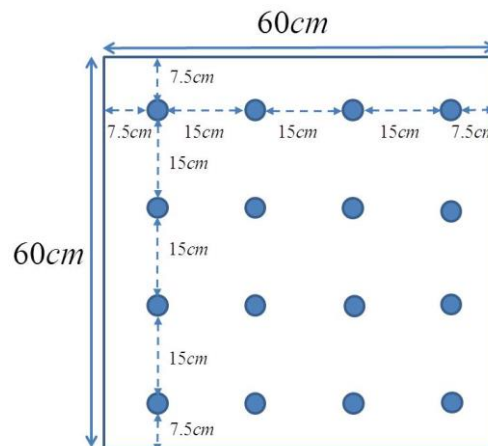


Fig. 1 Schematic of platform deck geometry and locations of the pressure transducers

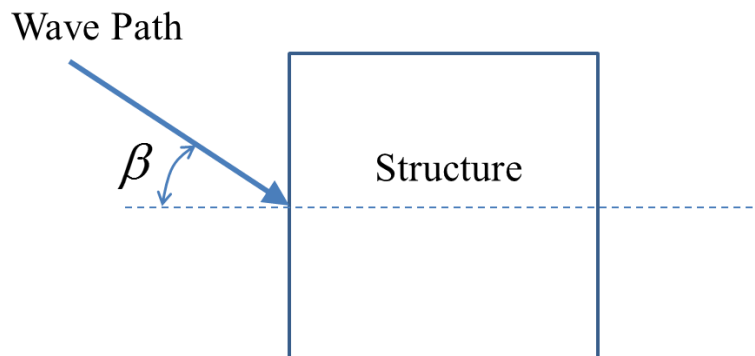
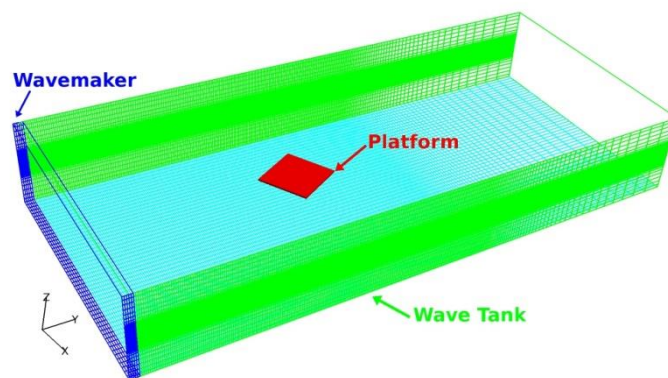


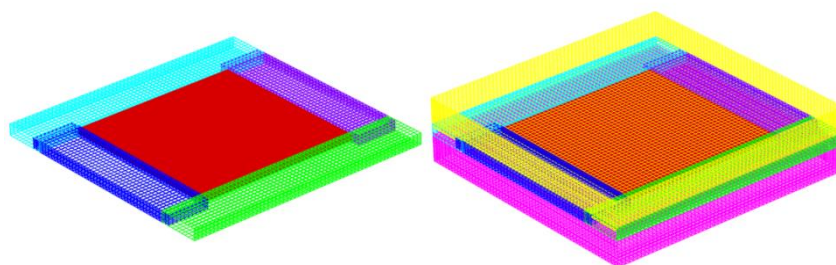
Fig. 2 Sketch of direction of wave propagation

The present numerical simulations were performed at full-scale using a constant time increment of $0.001T$ (1000 time steps per wave period). The water has a density of 1000 kg/m^3 and a dynamic viscosity of $1.12 \times 10^{-3} \text{ N}\cdot\text{s/m}^2$, while the air has a density of 1.23 kg/m^3 and a dynamic viscosity of $1.79 \times 10^{-5} \text{ N}\cdot\text{s/m}^2$. The effect of surface tension is neglected in the simulations, because its effect is insignificant in the large-scale fluid flow and has little contribution to slamming impact load. An overset grid system is employed to generate the appropriate grids for different directions of wave propagation. The overset grid system consists of eight computational blocks with a total of 1,197,627 grid points. In Fig. 3(a), one block grid with $51 \times 6 \times 81$ nodes plays the role of wave maker to generate the specified incoming wave. The incident regular waves are generated using the high order nonlinear wave theory of Cokelet (1977). One block grid with $51 \times 241 \times 81$ nodes serves as the wave tank for wave propagation. A numerical absorbing beach is applied in the downstream of the structure to prevent reflection waves.

The near-field region is consisted of another six-block grid (Fig. 3(b)), which is embedded in wave tank block grid. The platform deck is surrounded by two cubic grids on top and bottom, and four cubic grids on side. In this application, a series of cases with different directions of wave propagation are carried out. For the different cases, each of the block grids is kept in the same dimension, but the six-block near-field region is rotated by the direction of wave propagation. The size of these block grids are identical to the size used in experiment, but the center of platform deck is located at $x = 2.5 \text{ m}$, $y = 1.5 \text{ m}$ and above the mean water level.



(a) Grid for overall domain



(b) Grid for near-field region

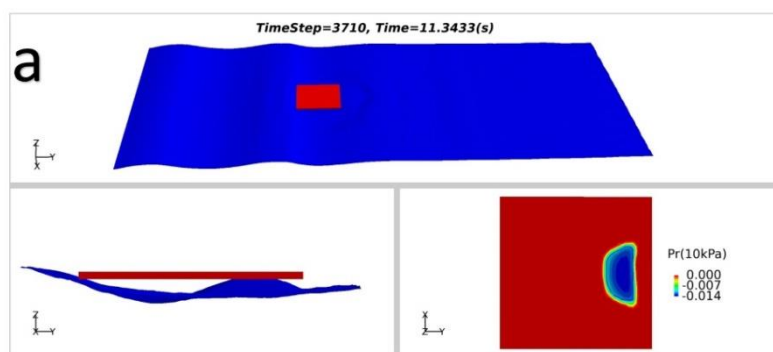
Fig. 3 Overset grid system

4. Results and discussions

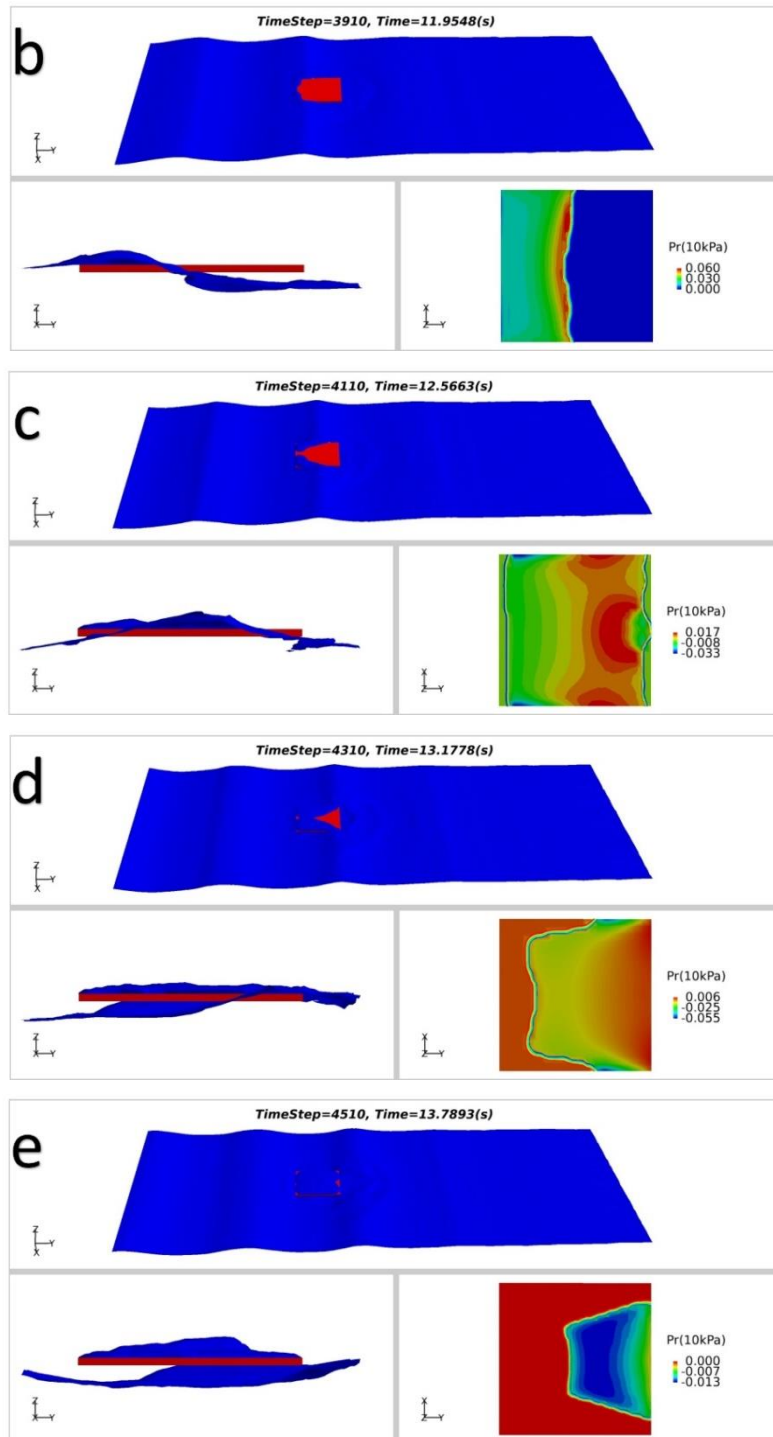
All of the simulations are normally performed for about 20 wave periods. The pressures at selected locations in Fig.1 are measured by the pressure sensors. The pressures in numerical results are scaled up to the experiment test and compared with the experimental data.

4.1 Case 1: 0 degree direction of wave propagation

The incoming waves are perpendicular waves to the structure when direction of wave propagation is 0° . Fig. 4 shows the snapshots of regular wave impingement on the 3D platform deck at six different time steps in top view and side view perspectives. Fig. 4 also shows the pressure contours on the underside of platform deck at the same time step. The incoming wave height H is 0.1 m, while the clearance of the underside of the structure above the mean water level s is 0.02 m which is lower than the wave crest. The wavelength L is 1.512 m, while the size of the structure is $0.6 \text{ m} \times 0.6 \text{ m}$ which can only occupy a portion of one complete wave. When the wave trough reaches the structure, there exists sufficient air gap between the underside of the deck and the free surface (Fig. 4(a)). The slamming impact can be avoided until the wave crest reaches the structure. The rising elevation of the wave not only impinges the underside of the deck (Fig. 4(b)), but also inundates some of topside deck region (Figs. 4(c)-4(e)). The impact loads keeps acting upon the deck until the water attached to the underside of the deck begins to recede. The water on the top of the deck continues the motion with its kinetic energy, and most of them falls down to the water from the sides of the deck (Fig. 4(f)). Moreover, the flow field in the downstream of the structure is also disturbed by the deck. The ripples can be observed behind the structure and follow the wave propagation to downstream. The snapshots of the pressure contours on the underside of the deck demonstrate the behavior of local impact pressure. When the wave surface is slamming on the deck and it is still rising, the up-lift impact pressure is dominated. The local impact pressure values are positive (Figs. 4(b) and 4(c)). As the wave crest recedes from the deck, the pressure turned to be significant negative value which represents the suction pressure (Fig. 4(e)). Furthermore, due to the suction pressure, the water attached to the deck underside is not easily separated from the deck wall (Figs. 4(a) and 4(f)). In addition, due to perpendicular wave in this case, the free surface flow patterns and pressure distribution contours exhibit the symmetrical patterns.



Continued-



Continued-

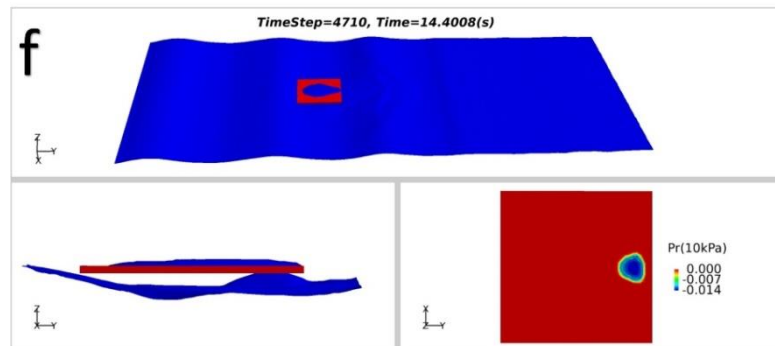
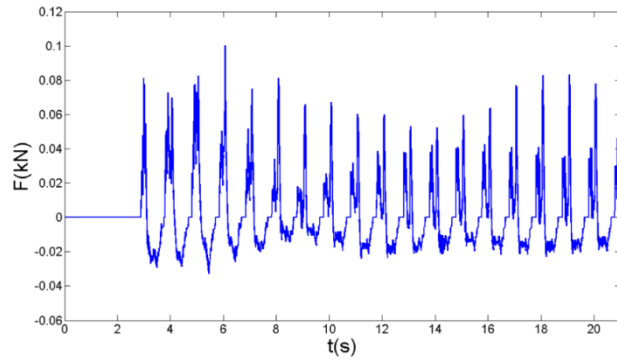


Fig. 4 Free surface patterns and underside of the deck pressure contours. (a) $t/T = 3.71$, (b) $t/T = 3.91$, (c) $t/T = 4.11$, (d) $t/T = 4.31$, (e) $t/T = 4.51$ and (f) $t/T = 4.71$

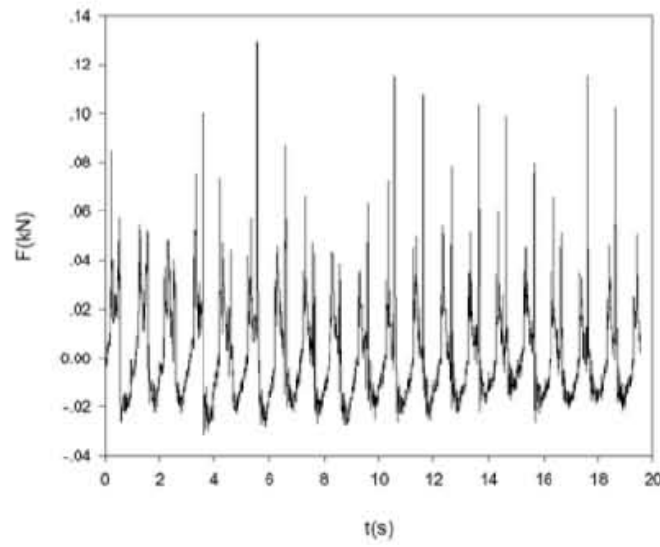
Fig. 5 shows the comparison of the total impacting force on the underside of the deck between numerical result and experimental data. The total force acting upon the bottom of the platform deck is calculated by integration of the pressures measured by 16 pressure transducers and the corresponding areas. It can be observed that the predicted impacting force time history is in good agreement with that measured by the experiment. In one slamming period, there is an impact force pattern followed by a negative suction force pattern. As discussed about the deck pressure contours above, the impact forces are due to the rising elevation of the free surface, and the suction forces are attributed to the water interface receding from the sub-face of the deck. More specifically, it can be seen that two impact force peaks exist in the same impact force pattern. After the initial force peak decays to nearly zero value, another fast-varying up-lift impact force with larger magnitude peak occurs. Although the second impact peak during different periods in experimental data show great instability due to the violent 3D free surface flow, the mean peak values are about 0.08 kN. The impact peaks predicted by numerical method are in close agreement with the experimental data. When it comes to the negative suction force, both the measured and predicted negative force peaks are close to about -0.02kN. Moreover, the time history of the impacting force behaves periodical due to the fact that the incoming wave is regular. The period in numerical data is about 1.0 s and it is also close to the period of the experimental time history.

4.2 Case 2: 30 degree direction of wave propagation

The incoming waves are oblique waves to the structure when direction of wave propagation is 30° . Fig. 6 shows the snapshots of regular wave impingement on the 3D platform deck in top view and side view perspectives, as well as the underside deck wall pressure contours. The free surface flow patterns are similar to those observed in Case 1. The slamming process also includes wave slamming (Fig. 6(b)), wave inundation (Figs. 6(c)-6(e)), and wave recession (Fig. 6(f)). The clear difference is that the incoming waves can climb up to the deck topside from two sides (Fig. 6(c)), since two deck edges are facing to the incoming wave. The pressure contours also display the impact or suction pressure at different time step. However, the free surface patterns and pressure contours are not symmetrical due to the platform deck orientation in this case.

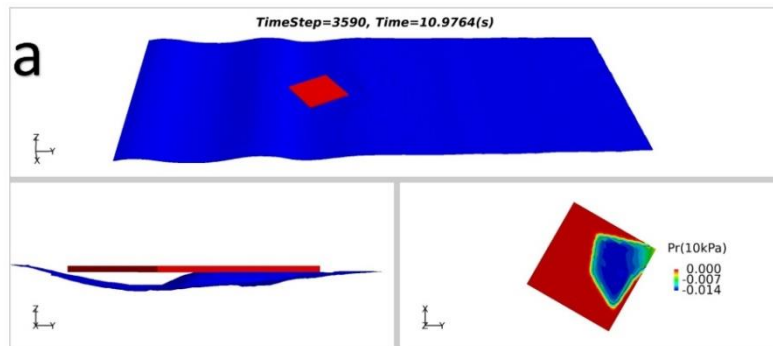


(a) Predicted impact force

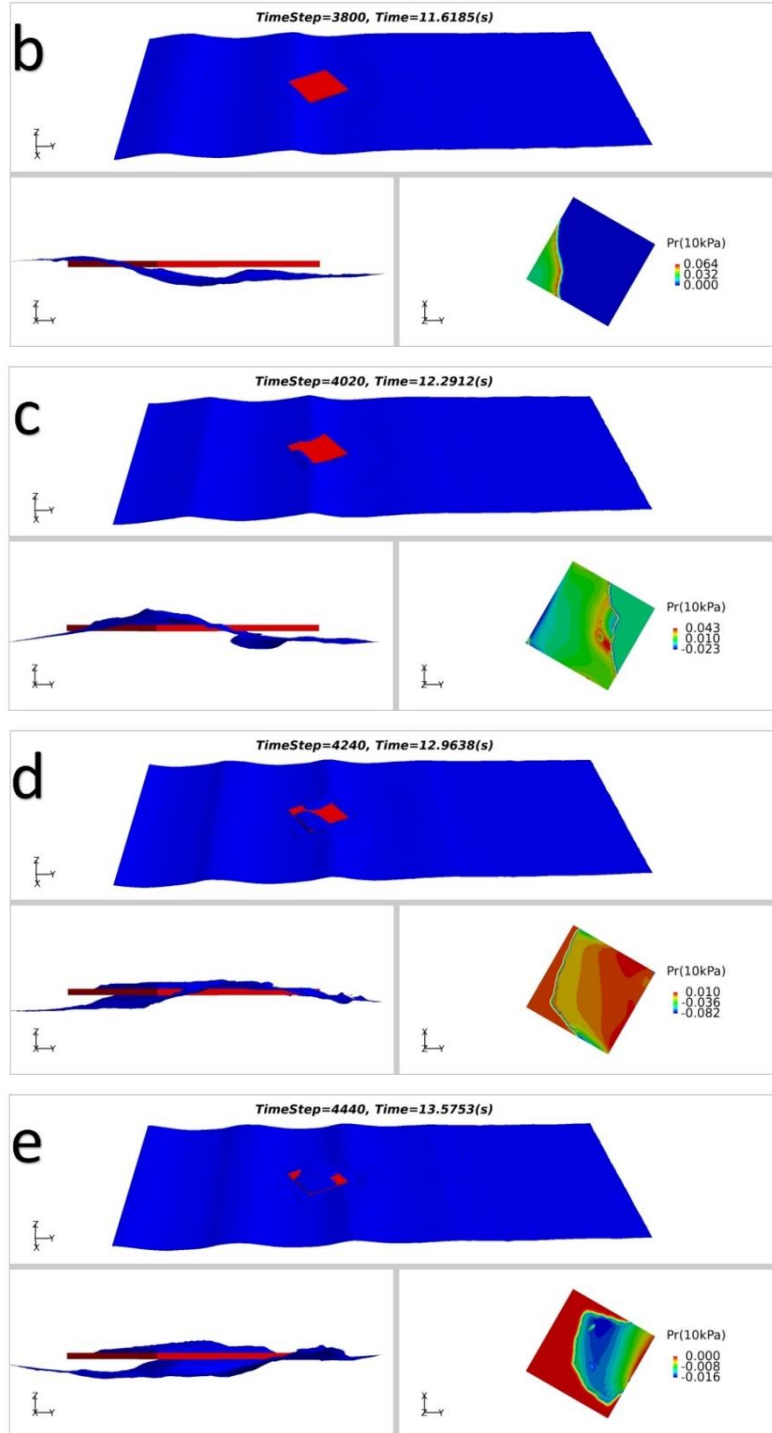


(b) Measured impact force

Fig. 5 Comparison of measured and predicted wave slamming impact forces in Case 1



Continued-



Continued-

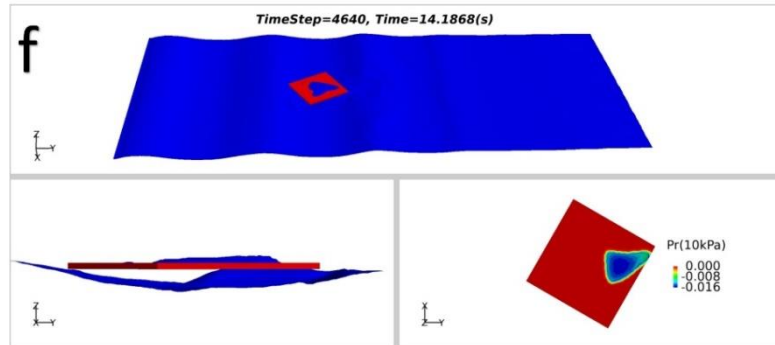
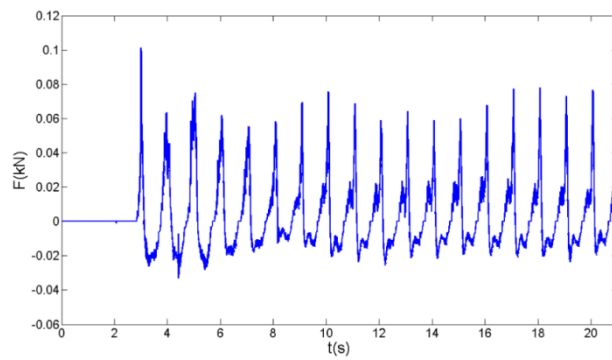
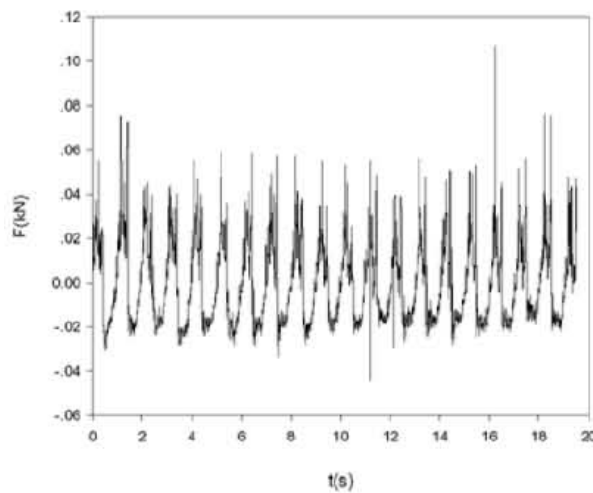


Fig. 6 Free surface patterns and underside of the deck pressure contours. (a) $t/T = 3.59$, (b) $t/T = 3.80$, (c) $t/T = 4.02$, (d) $t/T = 4.24$, (e) $t/T = 4.44$ and (f) $t/T = 4.64$



(a) Predicted impact force



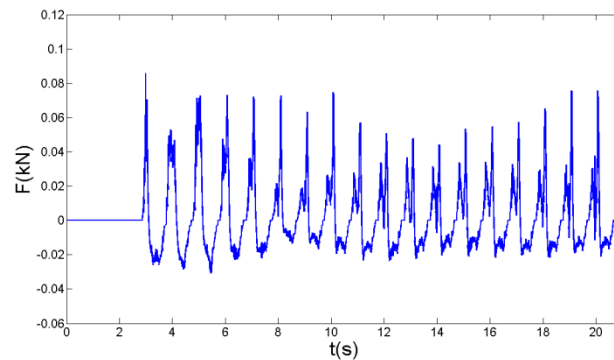
(b) Measured impact force

Fig. 7 Comparison of measured and predicted wave slamming impact forces in Case 2

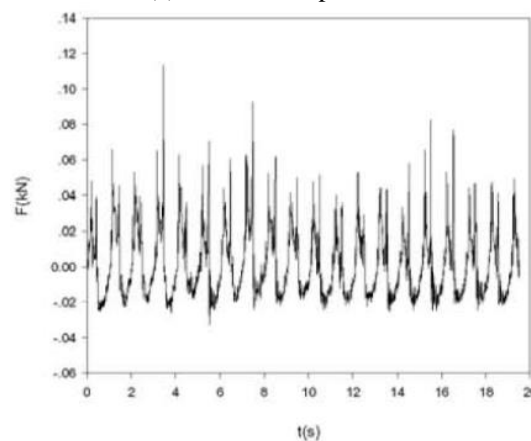
Fig. 7 shows the comparison of the total impacting force on the underside of the deck between numerical result and experimental data. The pattern of peak impact forces followed by suction forces still occurs in Case 2. Compared with measured impact force time history, although the first impact force peaks in the slamming periods are not fully developed, the second impact force peaks are in good agreement with the measured force peaks. In addition, the negative suction force peaks are close to -0.02 kN by the numerical method and experimental data.

4.3 Case 3 & Case 4: 15 degree & 45 degree direction of wave propagation

The incoming waves are also oblique waves to the structure when direction of wave propagation is 15° or 45° . As the free surface patterns in these two cases are very similar to those presented in Case 1 and Case 2, the detailed free surface patterns at different time steps in Case 3 and Case 4 are not presented here. The predicted wave slamming impact forces are still compared with the forces in experiment in Figs. 8 and 9, respectively. It can be observed that the peak impact forces and peak suction forces predicted by the CLSVOF method are in good agreement with those measured in experiment.

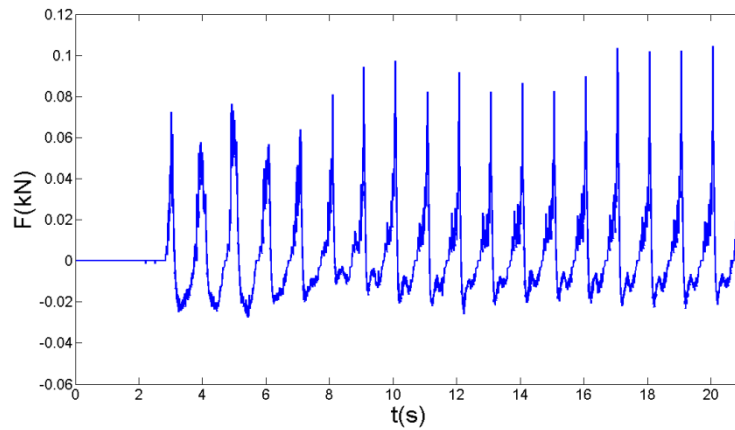


(a) Predicted impact force

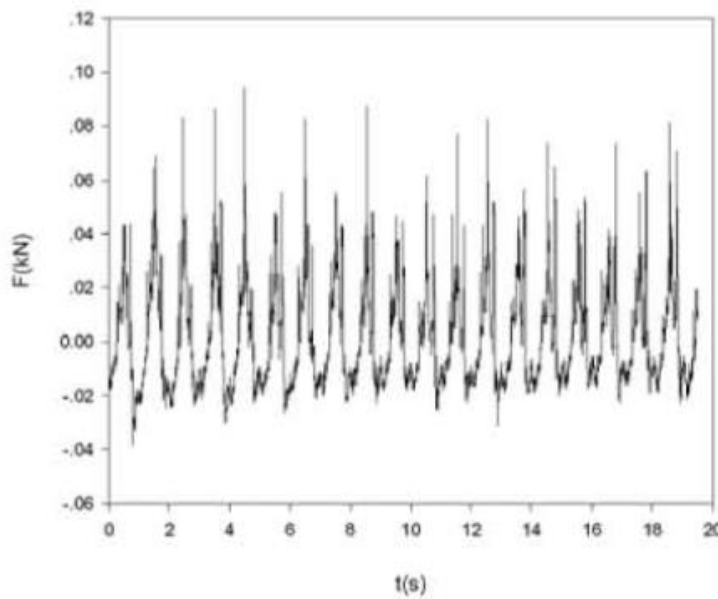


(b) Measured impact force

Fig. 8 Comparison of measured and predicted wave slamming impact forces in Case 3



(a) Predicted impact force



(b) Measured impact force

Fig. 9 Comparison of measured and predicted wave slamming impact forces in Case 4

5. Conclusions

In the present study, the CLSVOF method for an overset grid system has been implemented for the simulation of the regular wave impacting on the 3D offshore platform deck. The time history of impacting forces by the CLSVOF are in good agreement with the corresponding experimental data. Besides the impact forces are predicted by the present numerical method, the negative suction forces due to water receding are also accurately predicted. Moreover, the CLSVOF method has successfully captured many significant features of the flow patterns, including wave slamming,

wave inundation, and wave recession. The simulation results clearly demonstrate the capability of the present CLSVOF with an overset grid system for accurate prediction of the wave slamming on offshore structures.

References

- Broughton, P. and Horn, E. (1987), "Ekofisk Platform 2/4C: Re-analysis due to subsidence", *Proceedings of the Institution of Civil Engineers*, **82**(5), 949-979.
- Bunnik, B. and Buchner, T. (2007), "Extreme wave effects on deepwater floating structures", *Proceedings of Offshore Technology Conference*.
- Cokelet, E.D. (1977), "Steep gravity waves in water of arbitrary uniform depth", *Philo. T. R. Soc. A*, **286**, 183-230.
- Chen, H.C. (2010), "Time-domain simulation of nonlinear wave impact loads on fixed offshore platform and decks", *Int. J. Offshore Polar*, **20**, 275-283.
- Chen, H.C. (2011), "CFD simulation of compressible two-phase sloshing flow in a LNG tank", *Ocean Syst. Eng.*, **1**(1), 31-57.
- Chen, H.C. (2013), "CFD simulation of directional short-crested waves on Jack-up structure", *Int. J. Offshore Polar*, **23**, 38-45.
- Chen, H.C., Patel, V.C. and Ju, S. (1990), "Solutions of reynolds-averaged navier-stokes equations for three-dimensional incompressible flow", *J. Comput. Phys.*, **88**, 305-335.
- Chen, H.C. and Yu, K. (2009), "CFD simulations of wave-current-body interactions including greenwater and wet deck slamming", *J. Comput. Fluid*, **38**(5), 970-980.
- Gao, R., Ren, B., Wang, G. and Wang, Y. (2012), "Numerical modelling of regular wave slamming on subface of open-piled structures with the corrected SPH method", *Appl. Ocean Res.*, **34**, 173-186.
- Hirt, C.W. and Nichols, B.D. (1981), "Volume of fluid (VOF) method for the dynamics of free boundaries", *J. Comput. Phys.*, **39**, 201-225.
- Iwanowski, B., Grigorian, H. and Scherf, I. (2002), "Subsidence of the Ekofisk platforms: wave in deck impact study-various wave models and computational methods", *Proceedings of the 21th International Conference on Offshore Mechanics and Arctic Engineering*, January.
- Kaplan, P. (1992), "Wave impact force on offshore structures: re-examination and new interpretations", *Proceedings of Offshore Technology Conference*.
- Kaplan, P., Murray, J.J. and Yu, W.C. (1995), "Theoretical analysis of wave impact forces on platform deck structures", *Proceedings of the 14th International Conference on Offshore Mechanics and Arctic Engineering*, New York, USA.
- Osher, S.J. and Sethian, J.A. (1988), "Fronts propagating with curvature dependent speed: algorithms based on Hamilton-Jacobi formulations", *J. Comput. Phys.*, **79**, 12-49.
- Ren, B., Ding, Z., Wang, Y. and Ren, X. (2007), "Experimental study of regular wave impact on the three-dimensional structure in the splash zone", *Proceedings of the 17th International Offshore and Polar Engineering Conference*.
- Ren, B. and Wang, Y. (2004), "Numerical simulation of random wave slamming on structures in the splash zone", *Ocean Eng.*, **31**, 547-560.
- Sussman, M. and Puckett, E.G. (2000), "A coupled level set and volume-of-fluid method for computing 3d and axisymmetric incompressible two-phase flow", *J. Comput. Phys.*, **162**, 301-337.
- Wang, H. (1970), "Water wave pressure on horizontal plates", *J. Hydr. Eng. Div.*, **96**(10), 1997-2017.
- Zhao, Y. and Chen, H.C. (2013), "CFD simulation of violent free surface flows by a coupled level-set and volume-of-fluid method", *Proceedings of the 23rd International Offshore and Polar Engineering Conference*.
- Zhao, Y. and Chen, H.C. (2014), "Violent free surface flow simulations by a coupled level-set and volume-of-fluid method in overset grid systems", *Int. J. Offshore Polar*, **24**(2), 114-121.

Zhao, Y. and Chen, H.C. (2015), "Numerical simulation of 3D sloshing flow in partially filled LNG tank using a coupled level-set and volume-of-fluid method", *Ocean Eng.*, **104**, 10-30.